Transactions, SMiRT-24
BEXCO, Busan, Korea - August 20-25, 2017
Division V

UNDERSTANDING SEISMIC MOTION INCOHERENCY MODELING AND EFFECTS ON SSI AND SSSI RESPONSES OF NUCLEAR STRUCTURES

Dan M. Ghiocel[1] YoungSun Jang[2] and InHee Lee[3]

[1] President, Ghiocel Predictive Technologies, Inc., New York, USA (dan.ghiocel@ghiocel-tech.com)
[2] Professor, KEPCO E&C, Gimcheon, Korea (ysjang63@naver.com)
[3] President of CNG Softek Co. Ltd., Seoul, Korea (leeih@cngst.com)

MOTIVATION FOR THIS PAPER

Over the last decade we noticed that the seismic structural analysts often continue to have difficulties in understanding the motion incoherency modelling and evaluate correctly the motion incoherency effects on the SSI responses. This situation resulted due to the fact that most often structural analysts' background on the stochastic process or seismic wave modelling is quite limited. As result of the lack of background and unfamiliarity with the subject, many seismic analysts try to avoid considering the motion incoherency effects, basically ignore the physical reality. In contrast, other seismic analysts use crude simplifications on the mathematical modelling since for their limited understanding makes no difference. Such attitudes are obstacles for a faster progress for improving the accuracy of the seismic SSI analysis of nuclear structures. The paper addresses the key aspects related to the seismic motion incoherency modelling and effects on the SSI and SSSI responses of nuclear structures.

SEISMIC MOTION SPATIAL VARIATION IN HORIZONTAL PLANE

The spatial variation of the seismic ground motion in horizontal plane is caused by the complex wave propagation random pattern at a given site. In typical engineering terms, the seismic soil motion including spatial variation is called "incoherent" motion, while the seismic motion without any spatial variation is called "coherent" motion. It should be noted that the coherent motion is based on highly idealistic, 1D wave propagation models that assume that at any depth, the soil horizontal planes move as a "rigid" planes since all their all points have identical motions, as shown in Figure 1a. In contrast, the incoherent motion is based on real earthquake record databases from the dense arrays measurements in the free field, as shown in Figure 1b.

Basically, the incoherent motions for SSI analysis are stochastic simulations or realizations of real soil motions based on stochastic field models developed based on the statistical record databases. Incoherent motions are capable of simulating the complexity of the 3D wave propagation, implicitly including all types of incident seismic waves arriving at the nuclear facility site. Thus, the incoherent motions are more realistic idealizations of the seismic ground motions than the coherent motions that constrain all the soil points in a horizontal plane to move identical, so that each horizontal plane in the free-field soil deposit moves as a "rigid" plane.

For engineering applications, the motion spatial variation or motion incoherency is considered to be a superposition of two variation components due to i) the motion incoherency effects and ii) the wave passage effects. It should be noted that the incoherency and wave passage effects have qualitatively similar effects on seismic SSI analysis since both produce a lack of the spatial correlation between the soil motions at slightly different locations at the same depths. The incoherency variation produces motion amplitude random differences due to lack of similarity of the two motions, especially for the high-

frequency components, while the wave passage variation produces motion amplitude differences due to the time delay of between two identical motions.

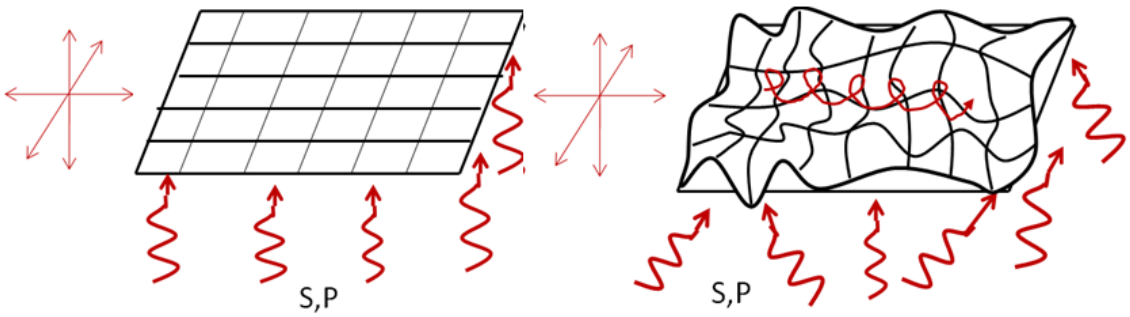

a) Coherent Waves b) Incoherent Waves

Figure 1. 1D Deterministic Coherent Waves vs. 3D Random Incoherent Waves

The main cause of the motion incoherency observed over distances of tens of meters that of interest for seismic SSI analysis is caused by wave scattering in the top 500 m of the soil/rock deposit (Abrahamson, 2007). The greater the variability of soil layering in horizontal direction, the higher the motion incoherency. In addition to the soil stiffness, the existing topographic features and the layered soil slopes are the most influential factors that can affect significantly the motion incoherency at a given site. For this reason it is desirable for a nuclear site to consider a site-specific coherence function, if the site includes significant topographic features, soil layering heterogeneities, or significant stiffness variation in the horizontal direction.

Typically, for horizontal layering and point sources, for which the scattering is mostly linear, it appears that the earthquake magnitude does not affect the motion incoherency. For large magnitudes at short distances is a significant increase of incoherency effects due to different wave paths from different parts of the fault rupture leading to larger deviation from single plane-wave propagation, such as it was observed at the 1995 Kobe earthquake. For other source parameters, such as focal mechanism and focal depth, no obvious effects on the motion incoherency were noticed.

The main influential factors that produce incoherency are:

- Soil profile stiffness variation in horizontal directions increases incoherency
- Soil layer inclination, local discontinuities, faults increase incoherency
- Topography features in vicinity could significantly increase incoherence
- Earthquake magnitude is less influential especially for single point source
- For short distances near faults, the multiple wave paths from different parts of fault rupture may drastically increase the spatial variations, both the motion incoherency and wave passage effects
- Focal mechanism and directivity apparently affect less incoherency

MATHEMATICAL MODELING OF SEISMIC MOTION SPATIAL VARIATION

The seismic wave field is idealized as a space-time stochastic process or a time-varying stochastic field model with zero-mean and Gaussian probability distribution that is completely described by its cross-spectral density function (CSD). This CSD function for two spatial soil locations i and j is computed based on the power-spectral density (PSD) functions at the two locations times the coherence function for the two locations:

$$S_{Uj,Uk}(\omega) = [S_{Uj,Uj}(\omega) S_{Uk,Uk}(\omega)]^{1/2} \Gamma_{Uj,Uk}(\omega) \quad (1)$$

The PSD functions describe the local random variations of the seismic soil motion for the two selected points i and j, while the coherence function describes the spatial variation of the seismic soil motion between points i to j. To describe the seismic ground motion spatial variation at a number of locations, the coherency matrix need to be defined.

The coherency matrix elements have a general form as follows

$$\Gamma_{Ui,Uk}(\omega) = \Gamma_{PW\,Ui,Uk}(\omega) \exp[i\omega(X_{D,i} - X_{D,k})/V_D] \quad (2)$$

in which the spatial coherence function at any frequency is computed by the product of the "plane-wave coherency" function (for random motion amplitude and phase variations) defined as a real positive function and the "wave passage" function (for deterministic motion phase variations) defined by a complex exponential function.

To simulate the seismic spatially varying motion stochastic field, as it is required as input for seismic incoherent SSI analysis, the most accurate and robust approach is the Monte Carlo simulation based on the Choleski decomposition or spectral factorization of the coherency matrix. The Monte Carlo simulation produces realistic random motion realizations in frequency domain with both random amplitudes and random phases as in the real earthquake records (Deodatis and Shinozuka, 1996, Ghiocel, 1996, 1998, 2004, Tseng, 1997).

Coherency Models

The separation distance and the frequency are the main influential parameters of the coherence function. The coherence function is defined as a 2D monotonically decreasing curve having the separation distance and the frequency as axis parameters. Figure 2 provides a visualization of the incoherent motion amplitude variation as a function of the wave component frequency or wavelength and relative distance between locations. Figure 2a shows a sketch illustrates the incoherent motion component variation for low and high frequencies, i.e. long and short wavelengths. Figure 2b shows a typical coherence function decaying with frequency and separation distance between locations (Abrahamson, 2007).

If there is no preferential incoherency direction for the ground motion variation, then, the coherence function is the same in all horizontal directions, so that the incoherent motion field is an "isotropic" or a "radial" stochastic wave field. Contrary, if there is a preferential incoherency direction, then, the coherence function is different for different directions, so that the incoherent motion wave field is an "anisotropic" or a "directional" stochastic wave field.

It should be noted that usually the coherence function at a given frequency depends only on the *separation distances* between different ground locations, but not on the absolute location positions. This implies that the stochastic motion field is also homogeneous, i.e. it has same statistics at any point in the horizontal plane.

Generic Coherence Functions

Based on a number of dense arrays earthquake records, Abrahamson provided two generic coherence functions, one for the soil sites and one for the rock sites. (Abrahamson, 2007). The Abrahamson coherency models are "generic" coherency models based on a set of statistical dense array records selected from different sites. The generic Abrahamson coherency models, as described in the 2007 EPRI

report (Short et al., 2007) does not include the motion directivity, being assumed as to be radial models with the same coherence function for all horizontal directions.

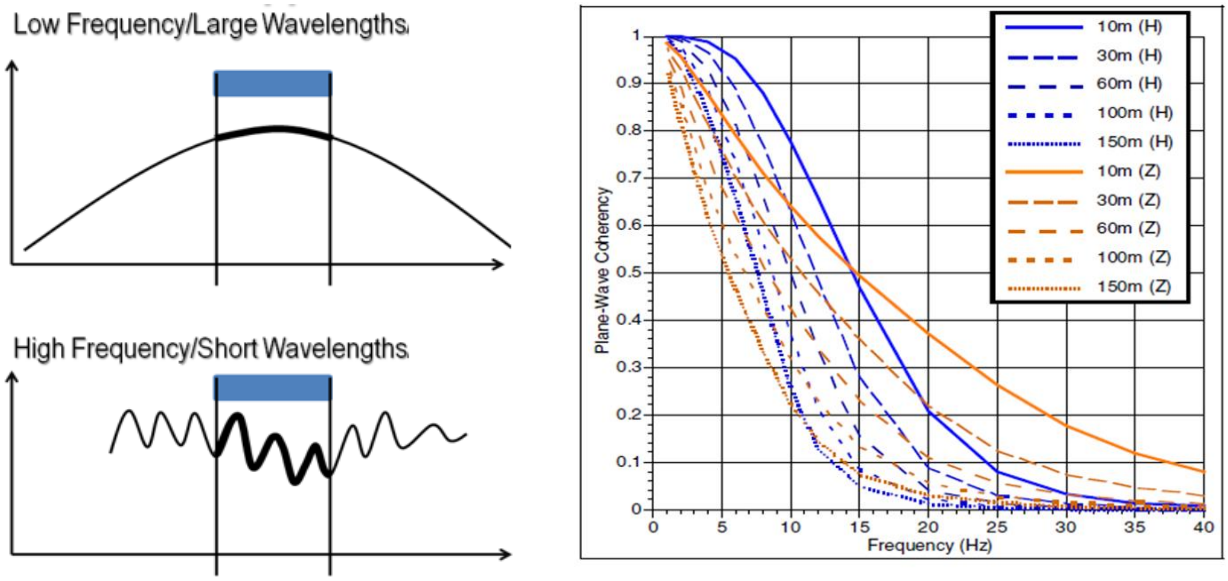

a) Incoherent Motion Amplitude Variation At Low and High Frequency

b) Smoothed Coherence Function for Horizontal and Vertical Motion Amplitudes (Abrahamson, 2007)

Figure 2 Incoherent Motion Amplitude Variation is A Function of Relative Distance and Frequency

These generic Abrahamson coherence functions were obtained for uniform horizontal soil layering sites with a gradual increase of the soil layer stiffness with depth. Most of the incoherent SSI analyses done in the past used the generic radial Abrahamson coherence models. However, more recently, some seismic experts questioned the applicability of the generic Abrahamson coherence functions to the site-specific applications, especially for sites that show quite different soil conditions than the site conditions used by Abrahamson for building the generic coherence function models for rock and soil sites (Abrahamson, 2007).

Site-Specific Coherence Functions

For site-specific applications, depending on the site seismological, geological and geotechnical characteristics, the use of the generic Abrahamson radial coherency models might not be appropriate. Figure 3 shows the site-specific coherence function in comparison with the generic Abrahamson coherence function computed for the Argostoli rock site recorded motion (Svay et al., 2016). The current trend for the site-specific applications is to use site-specific incoherency models, especially, if the selected site conditions include special features, as topography features, inclined soil layering, variable depth bedrock, or soil deposit discontinuities created by degraded soil lentils, local passive faults, or crushed soil bubbles that can significantly increase the motion incoherency effects. For sites close to faults, the multiple wave paths coming to the site location from different parts of fault ruptures may drastically increase both the motion incoherency and wave passage effects. This is typical situation for sites close to active faults.

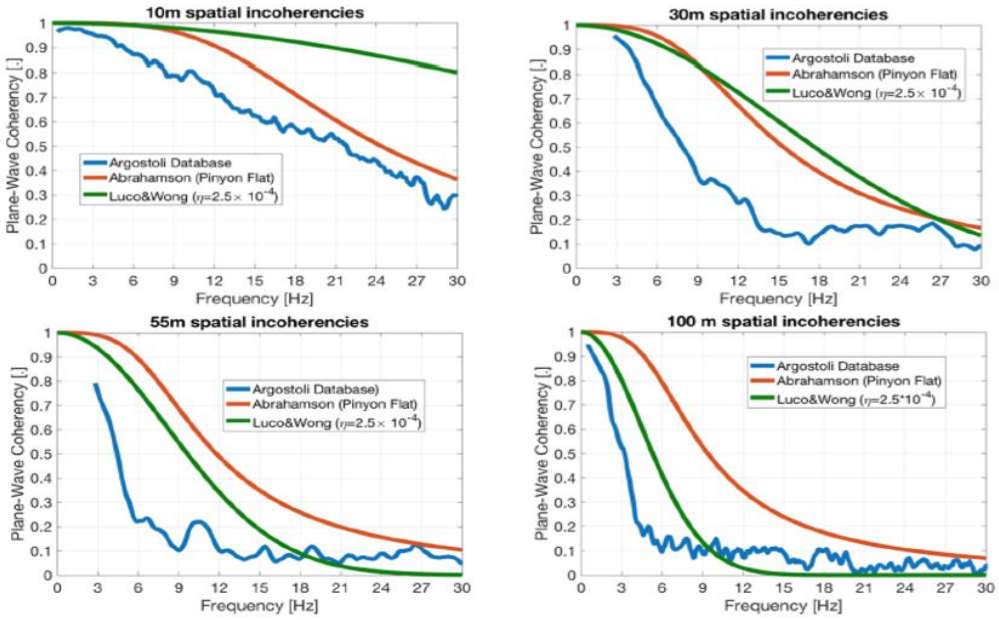

Figure 3 Site-Specific Coherence Function Computed for Argostoli Site (Svay et al., 2016)

Figure 4 shows a typical site-specific lagged coherence function estimated from records (Zerva, 2008). Figure 4a shows the role of smoothing in frequency on the coherence function estimate. The coherence estimates are obtained using the Hamming window with for the bandwidth parameter M= 1, 3, 5, 7 and 9. For no smoothing the coherence function is 1 for all frequencies. The larger the smoothing bandwidth is, the smaller the coherence estimate variance is. Abrahamson recommends the use of the parameter M=5 or 11-point Hamming window size (Abrahamson, 2007). It should be also noted that the lower the coherence value is at particular frequency, the larger the coherence estimate variance is (Ghiocel, 1996). Figure 4b shows the coherence mean estimate and with 95% confidence interval for a 11-point Hamming window.

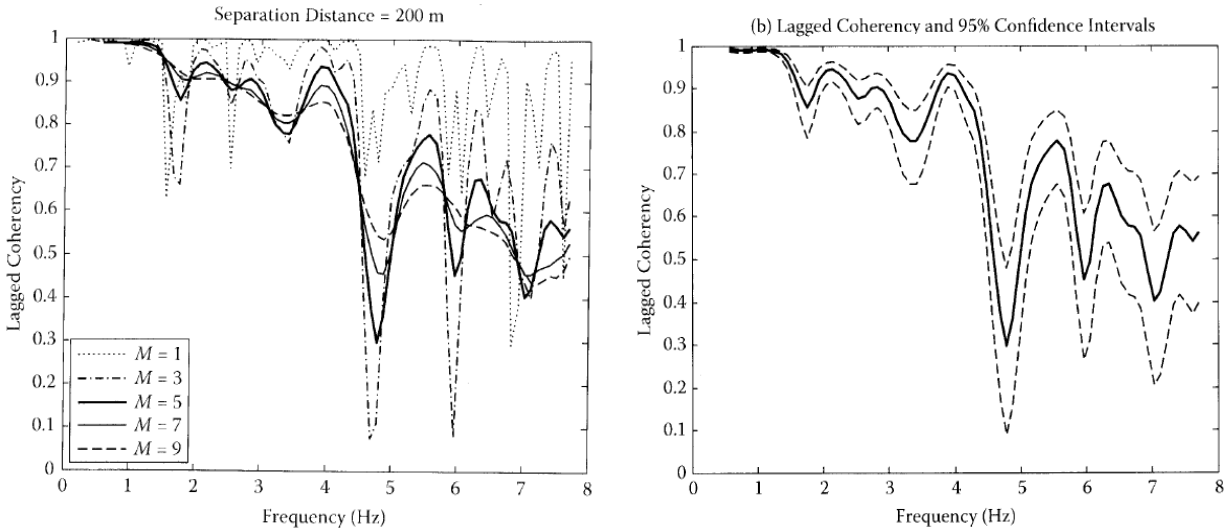

a) Coherence Estimate for Different Smoothings b) Coherence Mean and for 95% Confidence

Figure 4 Site-Specific Coherence Estimates for Different Smoothing Bandwidths Using Hamming Window (Zerva, 2008)

The site-specific coherence function shape in frequency depends on two types of random variations, coming from motion amplitude variations at the predominant soil deposit natural frequencies and the scattered energy effects in the soil media. The final site-specific lagged or plane-wave coherence function estimate, seen as an average estimate, should be much a smoothed curve not including the narrow band up-down-up random variations. Typically, the site-specific coherence models that are used in practice are smoothed, parametric plane-wave coherence function models, such as the EPRI Abrahamson coherence models developed for both the soil and rock sites, respectively, that are currently applicable to the seismic analysis of nuclear structures (Abrahamson, 2007).

The site-specific coherence functions can be also estimated based computational 2D (or 3D) nonlinear site response analysis based on probabilistic simulations as recommended in the USNRC RG1.208 guidance. The use the 3D site response analysis is at present time quite impractical due to the extensive field data collection and large computational efforts for a nuclear engineering project. The practical way for building site-specific coherence functions is to use of 2D site response analyses with probabilistic simulations for two or more horizontal directions as shown in Figure 5. The upper colored plot is a visualization of a part of about 1 km wide extracted from the 2D soil profile model that extends for few kilometers from the site in both left and right directions, plus having transmitting boundaries at the ends. The lower plots show the 2D soil motion for the same soil profile. The existence of non-vertically seismic waves due to the slightly inclined soil layering is quite visible. The effects of these randomly incident waves on the site motion is to increase the motion incoherency.

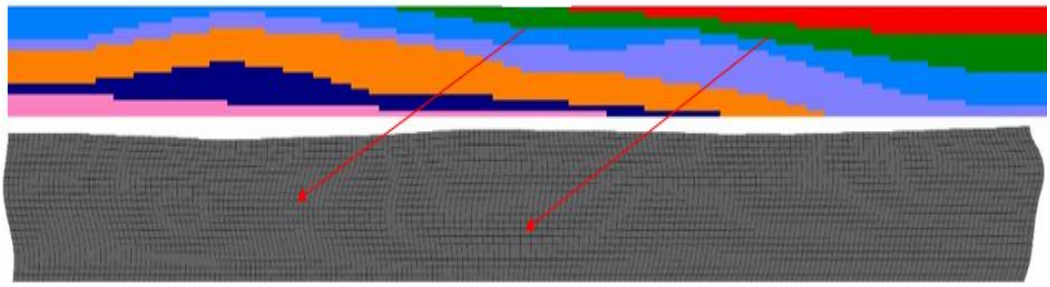

Figure 5 2D Probabilistic Soil Profile Model for Simulating Complex Wave Propagation

The site-specific coherence models can be quite different for slightly different site locations, and the simplified assumption of a homogeneous and isotropic incoherent wave field may not be applicable.

As an illustration of using probabilistic simulations to compute site-specific coherence functions, the Pinyon Flat rock site was considered. Using a 2D probabilistic FE model for the Pinyon Flat soil profiles the “site-specific” coherence functions based on probabilistic simulations were compared with the “generic” EPRI/USNRC accepted Abrahamson coherence functions based on the Pinyon Flat record database (Abrahamson, 2007). The 2D soil FE model size for the Pinyon Flat site is 1km long and 500m deep with both lateral and bottom transmitting boundaries. The soil mesh size was 5m for the horizontal direction and variable between 2.5m and 5m for the vertical direction. The Vs c.o.v. and D c.o.v. were 30%. The correlation length was taken 50m for horizontal direction and 25m for vertical direction, respectively. The statistical dependence between Vs and D was simulated by a correlation coefficient of -0.60. Figures 6 and 7 shows the Vs and D soil profile simulations for the Pinyon Flat site. The Vs and D random variations were assumed to follow the normal probability distribution.

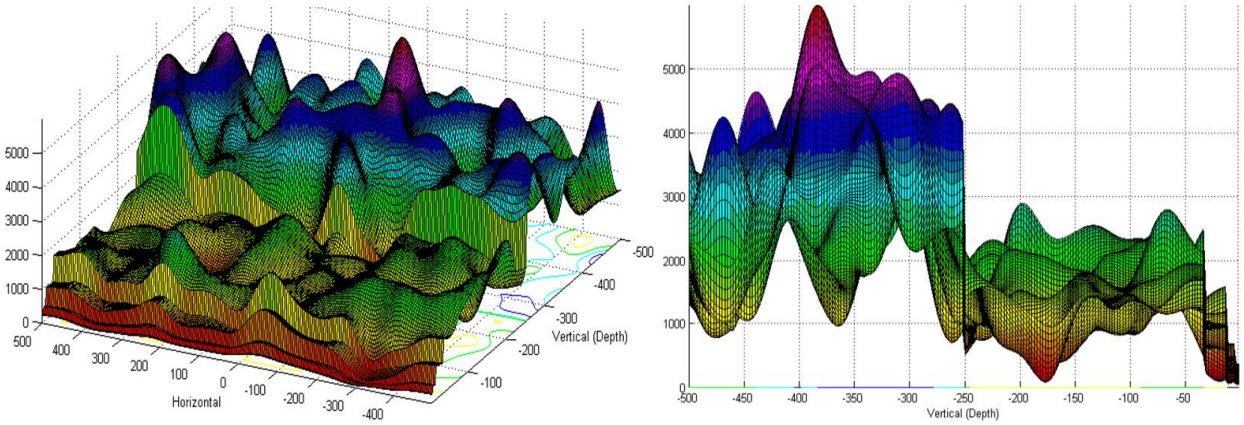

Figure 6 Pinyon Flat Simulated Vs Soil Profile; Axonometric View (left) and Lateral View (right)

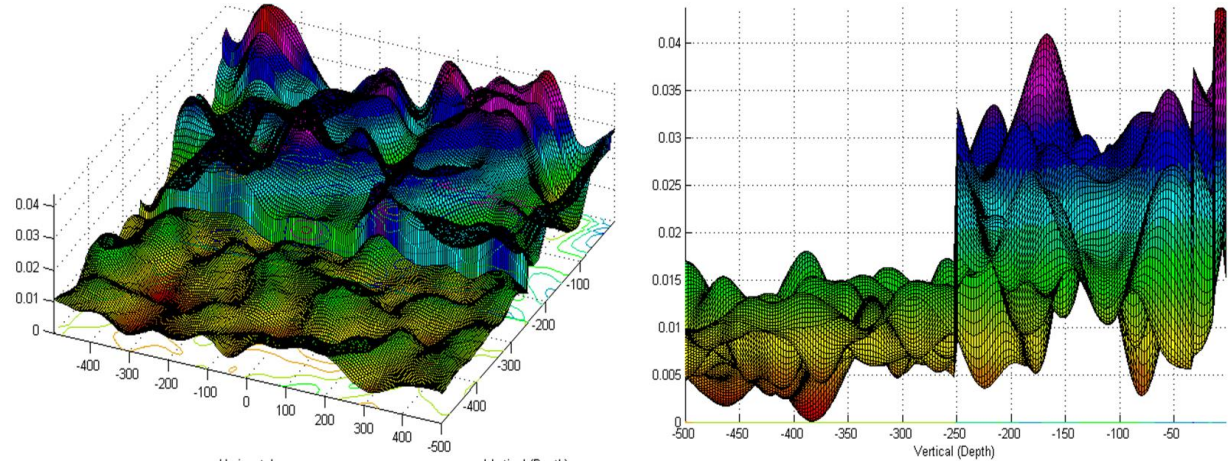

Figure 7 Pinyon Flat Simulated D Soil Profile; Axonometric View (left) and Lateral View (right)

Based on the 60 probabilistic site response simulations, the lagged coherence function at the site was estimated as shown in Figure 8 for 20m and 30m separation distances. Figure 9 shows the lagged coherence estimated based on the Pinyon Flat dense-array record database for 15m-30m separation distance range (Schneider, Stepp and Abrahamson, 1992, Zerva, 2008).

It should be noted that simulated lagged coherence function for the 20-30m separation distance based on the 2D probabilistic soil model and the estimated lagged coherence based on the dense array records for the 15m-30m range have a similar global variation over the 0-20 Hz frequency range, starting with the value of 1 at the zero frequency and ending with 0.60-0.65 at the 20 Hz frequency. The probabilistic site response simulations produce a slightly lower and slightly wavier coherence variation at lower frequencies due to the random variations of the sharp spectral peaks computed for the soil resonant frequencies using the 2D probabilistic soil model with the assumed parameters. However, other record-based lagged coherence estimates for two rock sites, as shown in Figure 9, indicate significantly lower values at the lower frequencies, and even lower than simulated coherences. The simulated lagged coherence functions compares well with the average of the lagged coherence functions based on the records at the three rock sites shown in Figure 9.

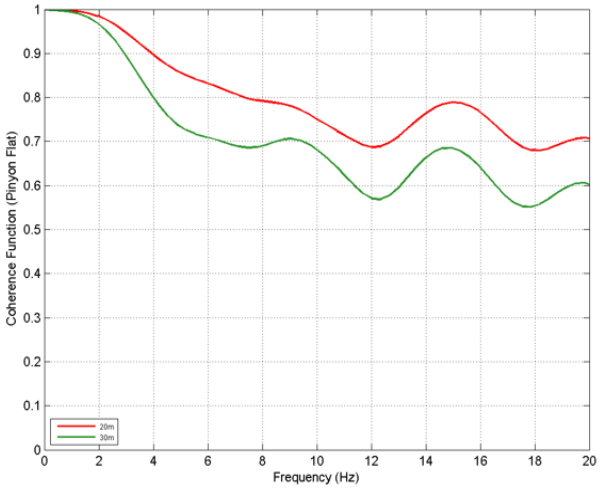

Figure 8 Simulated Coherences for 20m and 30m

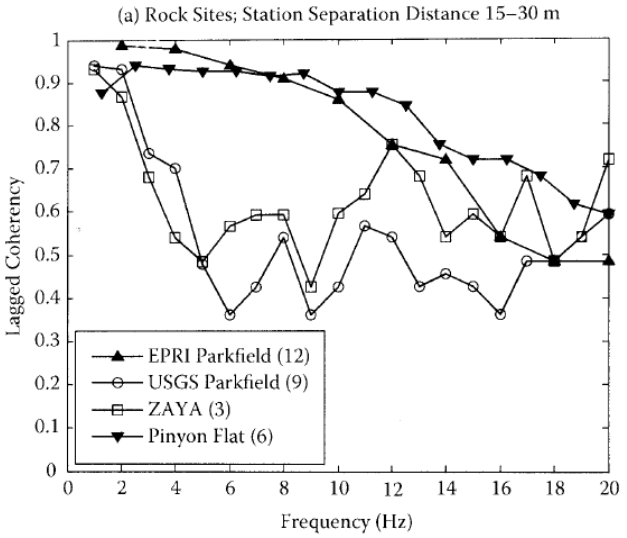

Figure 9 Record-based Coherences for 15-30 m

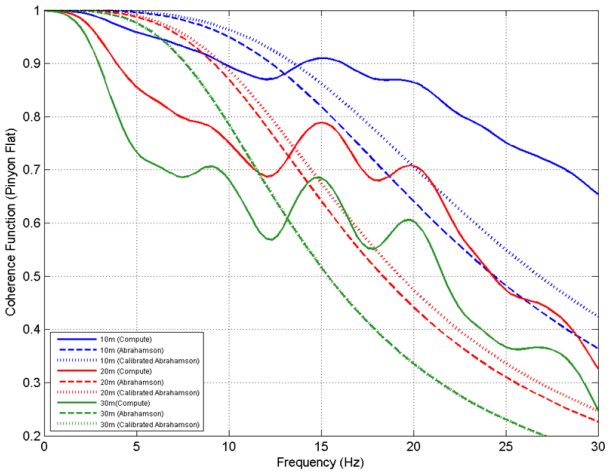

a) Simulated Lagged Coherence vs. Abrahamson Fitted P-W Coherence and EPRI P-W Coherence

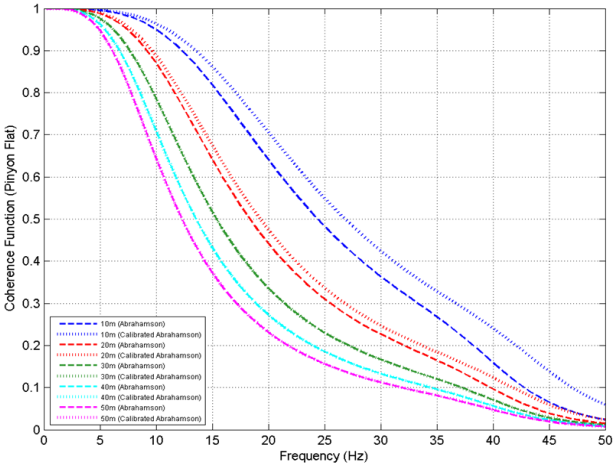

b) Abrahamson Fitted P-W Coherence vs. EPRI P-W Coherence for Rock Sites

Figure 10 Simulated Lagged Coherence (line) vs. Abrahamson Fitted Plane-Wave Coherence (dots) vs. EPRI/USNRC Accepted Abrahamson Plane-Wave Coherence for Rock Sites (dashed)

The final site-specific parametric plane-wave coherence function for the Pinyon Flat site was identified based on the simulated lagged coherence estimates. Figure 10a compares for the 10m, 20m and 30m separation distances, the simulated lagged coherence (line) against the final Abrahamson-fitted plane-wave coherence (dots) and the EPRI/USNRC accepted Abrahamson plane-wave coherence for rock sites (dashed) based on the Pinyon Flat record database (EPRI, 2007 and USNRC, 2008). It should be noted that the Abrahamson-fitted plane-wave coherence model was obtained by minimizing the numerical deviations between the analytical model and the simulated data in the interval 0-20 Hz. Beyond the 20 Hz frequency, the Abrahamson parametric plane-wave coherence models are extrapolated to go asymptotically to the zero value that is consistent with the scattered wave energy dissipation law in the infinite media.

Figure 10b compares for the 10m, 20m, 30m, 40m and 50m separation distances, the final site-specific Abrahamson-fitted plane-wave coherence model based on the 2D soil model probabilistic simulations, against the EPRI/USNRC accepted Abrahamson plane-wave coherence model that is currently considered in practice for all rock sites, and recently included in the ASCE 4-16 standard. It should be noted that for the 30m, 40m and 50m separation distances, the site-specific Abrahamson-fitted coherence based on simulations and the EPRI Abrahamson coherence based on the Pinyon Flat data records are fully overlapped.

SEISMIC INCOHERENT SSI ANALYSIS IMPLEMENTATION

Free-Field Incoherent Motion

The 1D wave propagation or coherent motion assumption has been accepted in the nuclear engineering practice over the last few decades. However, based on the 1D or vertically propagation assumption, the *coherent motion* at the ground surface or any depth is described by a "rigid body" plane motion in horizontal directions that is against the observation made in the field during earthquake events. This coherent motion implies that the soil motions for all points under the foundation footprint have identical motions. In contrast to simplified representation of seismic wave field by coherent motion, the *incoherent motion* is a more accurate representation of the seismic random wave field that realistically includes the 3D seismic wave propagation aspects. Incoherent motions implicitly incorporate randomly inclined body waves and surface waves since they are developed based on real data from the dense array statistical earthquake records. Incoherent motions represent realistic 3D wave motion simulations based on the stochastic models which are developed from real record databases. Thus, incoherent motions include a much more realistic idealization of seismic ground motion than coherent motions.

To capture this spatial variability of the ground motion, an adequate stochastic field model is required. Assuming that the spatial variation of the ground motion at different locations could be defined by a homogeneous/stationary Gaussian stochastic field, then, the spatial variability is completely defined by its coherency spectrum or coherence function.

The coherent free-field motion at any interaction node dof k, $U_k^{g,c}(\omega)$ is computed by

$$U_k^{g,c}(\omega) = H_k^{g,c}(\omega) U_0^g(\omega) \tag{3}$$

where $H^{g,c}(\omega)$ is the (deterministic) complex coherent ground transfer function vector at interface nodes and $U_0^g(\omega)$ is the complex Fourier transform of the control motion.

Similarly, the incoherent free-field motion at any interaction node dof k, $U_k^{g,i}(\omega)$ is computed by:

$$U_k^{g,i}(\omega) = \tilde{H}_k^{g,i}(\omega) U_0^g(\omega) \tag{4}$$

where $\tilde{H}^{g,i}(\omega)$ is the (stochastic) incoherent ground transfer function vector at interaction node dofs and $U_0^g(\omega)$ is the complex Fourier transform of the control motion. The main difference between coherent and incoherent free-field transfer function vectors is that $H^{g,c}(\omega)$ is deterministic quantity while $\tilde{H}_k^{g,i}(\omega)$ is a stochastic quantity (the tilda represents a stochastic quantity). The $\tilde{H}_k^{g,i}(\omega)$ quantity includes deterministic effects due to the vertically propagating body waves adjusted to incorporate the stochastic motion spatial variation effects in the horizontal plane. Thus, the incoherent free-field transfer function at any interaction node can be defined by:

$$\tilde{H}_k^{g,i}(\omega) = S_k(\omega) H_k^{g,c}(\omega) \quad (5)$$

where $S_k(\omega)$ is a frequency-dependent quantity that includes the effects of the stochastic spatial variation of free-field motion at any interaction node dof k due to incoherency. In fact, in the numerical implementation based on the complex frequency approach, $S_k(\omega)$ represents the complex Fourier transform of relative spatial random variation of the motion amplitude at the interaction node dof k due to incoherency. Since these relative spatial variations are random, $S_k(\omega)$ is stochastic in nature. The stochastic $S_k(\omega)$ can be computed for each interaction node dof k using the *spectral factorization* of coherency matrix computed for all SSI interaction nodes. For any interaction node dof k, the stochastic spatial motion variability transfer function $\tilde{H}_k^{g,i}(\omega)$ in complex frequency domain is described by the product of the stochastic eigen-series expansion of the spatial incoherent field times the deterministic coherent ground motion complex transfer function:

$$\tilde{H}_k^{g,i}(\omega) = [\sum_{j=1}^{M} \Phi_{j,k}(\omega) \lambda_j(\omega) \eta_{\theta j}(\omega)] H_k^{g,c}(\omega) \quad (6)$$

where $\lambda_j(\omega)$ and $\Phi_{j,k}(\omega)$ are the j-th eigenvalue and the j-th eigenvector component at interaction node k. The factor $\eta_{\theta j}(\omega)$ is the random phase component associated with the j-th eigenvector that is given by $\eta_{\theta j}(\omega) = \exp(i\theta_j)$ in which the random phase angles are assumed to be uniformly distributed over the unit circle.

Incoherent SSI Response Motion

For incoherent motion input, the complex Fourier SSI response at any structural dof i, $U_i^{s,i}(\omega)$, is computed similarly by the superposition of the effects produced by the application of the incoherent motion input at each interaction node dof k:

$$U_i^{s,i}(\omega) = \sum_{k=1}^{N} H_{i,k}^{s}(\omega) U_k^{g,i}(\omega) = \sum_{k=1}^{N} H_{i,k}^{s}(\omega) [\sum_{j=1}^{M} \Phi_{j,k}(\omega) \lambda_j(\omega) \eta_{\theta j}(\omega)] \, H_k^{g,c}(\omega) U_0^{g}(\omega) \quad (7)$$

Based on the approximation of the above equation, various incoherent SSI prediction approaches, from refined stochastic simulation approaches to simpler deterministic approaches, were implemented within the SASSI framework. The stochastic simulation approach based on Monte Carlo simulation provides a "theoretical exact" approach, while all other deterministic approaches that include simplified assumption of motion amplitude and phasing are "approximate" approaches that needs to be used for any nuclear project with cautiousness after their validation against the stochastic simulation approach.

The number of coherency modes has a significant impact on the incoherent SSI responses, especially on ISRS. These coherency modes are the eigen-modes of the coherency matrix computed for the interaction nodes. The total number of coherency modes is equal to the number of interaction nodes. Herein, a convergence criterion for the eigen-mode expansion is presented. This convergence criterion is accepted in the US practice to check the minimal number of coherency matrix spatial modes that needs to be included in SSI analysis.

It should be noted that the stochastic simulation approach based on Monte Carlo simulation include automatically of the coherency matrix nodes. The mode expansion criterion is applicable to the deterministic SRSS approaches.

At each frequency, the free-field plane-wave coherency matrix $\mathbf{\Sigma}$ that is similar to a correlation matrix and is positive-definite is decomposed using spectral factorization in a set of real eigenvectors, as follows:

$$\mathbf{\Sigma} = \mathbf{\Phi}\mathbf{\Lambda}^2\mathbf{\Phi}^T \tag{8}$$

where $\mathbf{\Lambda}^2$ and $\mathbf{\Phi}$ are the diagonal eigenvalue matrix and the eigenvector matrix of the coherency matrix at given frequency. If the coherency matrix has a size of N x N, then, the free-field motion coherency matrix is fully reconstructed using spectral factorization only if all eigenvectors are used. *If only a fraction of the eigenvectors are considered then the free-field coherency matrix is only approximated.*

To check the eigen-expansion convergence criterion the norm of the trace of the transformed matrix $\mathbf{\Lambda}^2$ and the norm of the trace of the original $\mathbf{\Sigma}$ that are both equal to N, the number of interaction nodes are used. The diagonal elements of the two matrices have all a unit value, i.e. for zero distance between two locations, the coherent function has value 1 for any node location.

Thus, for a given frequency, if *all* incoherent eigenvectors (modes) are considered, then, the following equality shall hold

$$\sum_{j=1}^{N} \lambda^2{}_j = N \tag{9}$$

It should be noted the eigenvalue $\lambda^2{}_j$ correspond to the variance associated to the mode shape j, while N corresponds to the total variance of the incoherent amplitude variation field at given frequency. If only *a reduced number* of modes are used, say m < N, then, the total variance of the incoherent amplitude variation field will be not recovered since

$$\sum_{j=1}^{m} \lambda^2{}_j < N \tag{10}$$

The percent contribution of mode j to the total incoherent field variance is given by

$$\upsilon_j = \frac{\lambda^2{}_j}{N} 100 \tag{11}$$

For m incoherent modes that are ordered with increasing contribution, the cumulative modal contribution (in %) of total variance of the wave field variance is calculated by

$$\sum_{j=1}^{m} \upsilon_j = \sum_{j=1}^{m} \frac{\lambda^2{}_j}{N} 100 \tag{12}$$

The above equations are to check the coherency mode expansion convergence.

In practice, these cumulative modal contributions should be at least 90% to ensure a reasonable mode expansion convergence criterion is used. This 90% criterion is a similar to the convergence criterion of the 90% cumulative modal mass contribution used in structural dynamics that is recommended by the ASCE 4-16 standard in Section 3. This criterion is important only when the deterministic SRSS approach is applied. This convergence checking is not necessary for the stochastic simulation approach that includes all N coherency modes, so that the mode expansion is fully converged.

Incoherent SSI Stochastic and Deterministic Approaches

In 2007, EPRI investigated different incoherent SSI approaches for their application to the new nuclear power plant design within the United States (Short, Hardy, Merz and Johnson, 2007). Both stochastic and deterministic incoherent SSI approaches were considered. The stochastic approach that is the "theoretically exact" approach was considered to be the most accurate and robust, and the reference approach. Other deterministic approaches were compared against the stochastic approach results.

Stochastic approach is based on the Monte Carlo simulation of a set of incoherent motion field random realizations. Using Stochastic Simulation (Simulation Mean in EPRI studies) algorithm, a set of incoherent motion random samples are generated at the SSI interaction nodes. For each incoherent motion random sample a new seismic load vector is computed. The mean SSI response is obtained by statistical averaging of SSI response random samples.

Deterministic approaches used were based on using simple superposition rules of random incoherent mode effects, such as the Algebraic Sum (AS, in 2007 EPRI studies) or the Square-Root of the Sum of Square (SRSS, in 2007 EPRI studies), to approximate the mean incoherent SSI motion.

It should be noted that the 2007 EPRI (Short et al. 2007) validated approaches are based on an *"industry consensus*" based on SSI results obtained for simple stick models with rigid basemats. At that time, the EPRI industry team uses the ACS SASSI, ClassiInco and SASSI Bechtel codes for a simple RB stick model with a rigid basemat. To fully match the *"industry consensus"* results based on the simple, approximate SRSS zero-phase approaches, the rigorous Stochastic Simulation (SS) approach has to be applied by the EPRI project researches using the "phase adjustment" option that basically was zeroing the complex response phasing. However, it should be understood that by neglecting the complex random phasing, the incoherent SSI responses are less incoherent, and by this creates an artificial bias toward coherent responses.

For rigid foundations, the effect of soil motion phasing is much less significant, since the rigid foundations due to kinematic interaction effects filter out all the coherency matrix high-order modes that correspond to wavy mode shapes. For flexible foundations, the zero-phasing is usually conservative, but not always (Ghiocel, 2015). It should be understood that for FE models with elastic foundations, rather than stick models with "rigid" foundations, the existing deterministic SSI approaches based on the zero-phase assumption, either AS or SRSS, always loose a part of the real physics, and, therefore, should be always suspected for potentially producing some crude ISRS results (Ghiocel, 2014, 2015, 2016).

An additional limitation of the EPRI zero-phase approaches is that the incoherent SSI response time histories are not usable for the multiple time-history analysis of secondary systems. The cross-correlation between SSI motions at different locations are largely affected by zeroing the SSI response motion phases.

Particular Implementations in ACS SASSI

The ACS SASSI software includes all the incoherent SSI approaches validated during the 2007 EPRI studies, plus a number of alternate approaches. The stochastic simulation approach can be applied with or without phase adjustment. Also, the SRSS approach can be applied with zero-phase as in the 2007 EPRI studies, or with coherent non-zero phase instead of the zero-phase that represents a correction to the initial SRSS approach used by EPRI.

In the specific context of the SASSI methodology, the motion incoherency effects on are included by randomization of the seismic load vector. Two alternate approaches were implemented based on the randomization of 1) the free-field seismic load vector (FFL) and 2) the free-field motion vector (FFM). The FFL approach was validated in the EPRI studies (Short et al., 2007).

Assuming that the incoherent random variation (scale) vector obtained by the coherence matrix spectral factorization is denoted by $\boldsymbol{\varepsilon}(\omega)$, and the soil impedance matrix and free-field motion are denoted by $\mathbf{X}_{\mathrm{f}}(\omega)$ and $\mathbf{U}_{\mathrm{f}}(\omega)$,respectively, then, the two alternate approaches for defining the incoherent seismic load vector, $\mathbf{F}_{\mathrm{f}}^{\mathrm{inc}}(\omega)$, acting at the interaction nodes, are described as follows:

For the FFL approach, the incoherent seismic load vector is computed based on the randomization of the coherent seismic load vector:

$$\mathbf{F}_{\mathrm{f}}^{\mathrm{inc}}(\omega)=\mathbf{X}_{\mathrm{f}}^{\mathrm{coh}}(\omega)\mathbf{U}_{\mathrm{f}}^{\mathrm{inc}}(\omega)=\boldsymbol{\varepsilon}(\omega)[\mathbf{X}_{\mathrm{f}}^{\mathrm{coh}}(\omega)\mathbf{U}_{\mathrm{f}}^{\mathrm{coh}}(\omega)] \tag{13}$$

in which the $\boldsymbol{\varepsilon}(\omega)$ is the randomization vector that is applied element by element to the seismic load vector.

For FFM approach, the incoherent seismic load vector is computed based on the randomization of the coherent free-field motion vector

$$\mathbf{F}_{\mathrm{f}}^{\mathrm{inc}}(\omega)=\mathbf{X}_{\mathrm{f}}^{\mathrm{coh}}(\omega)\mathbf{U}_{\mathrm{f}}^{\mathrm{inc}}(\omega)=\mathbf{X}_{\mathrm{f}}^{\mathrm{coh}}(\omega)[\boldsymbol{\varepsilon}(\omega)\mathbf{U}_{\mathrm{f}}^{\mathrm{coh}}(\omega)] \tag{14}$$

None of the above approaches is “theoretically exact”, although the FFM approach may appear to be closer to the “physics”, but realistically is not, as explained below.

The FFL approach uses the coherence matrix eigen-expansion randomization applied directly to the coherent free-field seismic load vector. Apparently, this approach misses randomizing some parts of the seismic load vector elements related to the coupling terms of the soil impedance matrix. The non-randomized elements are related to the coupling terms of the “coherent” impedance matrix that are different from the coupling terms elements of the “incoherent” impedance matrix. Since the “incoherent” impedance matrix is not available, it is approximated by the “coherent” impedance matrix. This is a slight disconnect from the real wave propagation physics that is accepted in practice. The FFL approach is applicable to both surface and embedded structures.

The FFM approach uses the coherence matrix eigen-expansion randomization applied to the coherent free-field motion vector. This approach is closer to “theory”, if and only if, the exact incoherent impedance matrix based on a physics-based model consistent with the incoherent free-field motion is available, which is not. Because of the use of the coherent impedance matrix as an approximation, some numerical noise is included in the wave scattering calculations. It should be noted that these

approximation differences in the soil impedance matrix coupling terms can slightly affect the local wave propagation pattern by introducing some an artificial wave scattering noisy effect for the embedded structures. For this reason, the FFM approach is not recommended for embedded structures.

The two approaches provide same or very close results for stick SSI surface models with rigid basemats, as used in the 2007 EPRI validation studies (Short et al., 2007). However, for the deeply embedded models, the use of the FFM approach in conjunction with the Abrahamson isotropic coherence models (with a radial coherence function for all directions), appears to artificially increase the motion incoherency effects. The FFM approach may generate slightly different excavated soil solutions for the Flexible Volume (FV) method versus the Flexible Interface (FI-EVBN, or the Modified Subtraction method, MSM). The FFM approach with the FV method may produce larger wave scattering effects due to an over randomization of the scattered wave propagation. Some quantitative comparative results using the FFL and FFM approaches in conjunction with the FV and FI-EVBN (or MSM) are included in the next section. Both surface and embedded RB complex models are considered.

The effect of motion incoherency directionality was not investigated in the 2007 EPRI studies. However, this motion incoherency directionality can affect the SSI responses. In ACS SASSI, the motion incoherency directionality is described in terms of the coherence function variation in the horizontal plane, i.e. the orientation and shape of the correlation ellipse. If the relative distances denoted by DX and DY correspond to the relative distances between any pair of interaction nodes in the principal direction of motion, denoted by X direction and the Y direction, respectively, then, an alpha directionality factor can be defined used to handle the motion incoherency directionality that is described by the shape of the coherence ellipse for the principal directions of motion, the X and Y axis, if angle of line D with X axis is zero, or the line D and the line perpendicular to line D, if angle of line D with X axis is not zero. The role of alpha factor is shown in Figure 11.

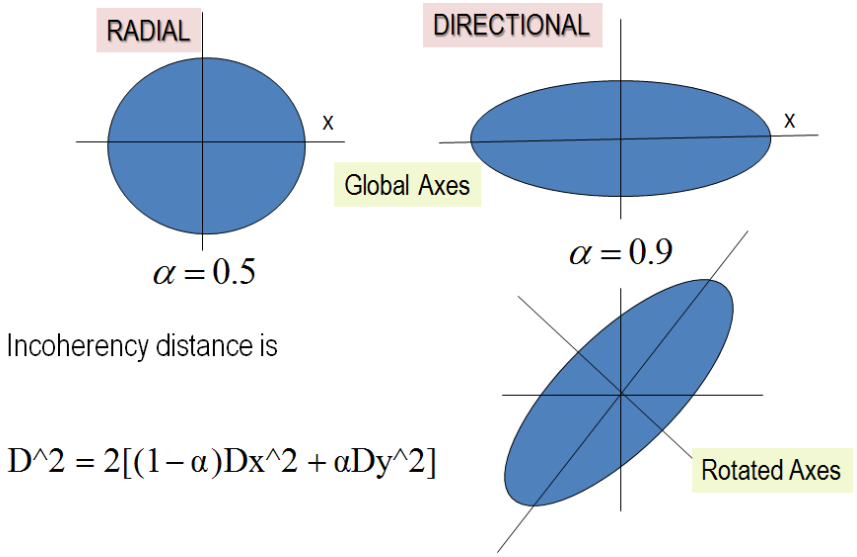

Figure 11 Role of Alpha Direction Factor on Motion Coherence Function Amplitude Variation in Horizontal Plane (Changes in Ellipse Shape)

The relative distance D between each pair of interaction nodes is used to compute the free-field coherence matrix. The relative distance D is determined for each pair of interaction nodes based on the component distances between the two paired nodes parallel with the X and Y axes, DX and DY, via a homotopic transformation that weighs the projected distances, as desired by the user, as follows:

$$D = \mathrm{sqrt}\,(2[(1-\alpha)DX\text{^}2 + \alpha DX\text{^}2]) \quad (15)$$

The above equation makes possible to introduce the motion coherence directivity aspects. If alpha factor is equal to 0, only the relative distances parallel with X axis matters, while if alpha factor is equal to 1, ten, only the relative distances parallel with X axis matters. The radial model is obtained when alpha factor is equal to 0.50 that indicates that the relative distances parallel with X axis and parallel to Y axis have identical weights. For the 0.50 parameter value, the relative distance D is equal to the real geometric distance between the two paired interaction nodes. Quantitative comparisons for the motion incoherency directionality/directivity effects are included in the next section.

MOTION INCOHERENCY MODELING ISSUES

In this section the impact of different motion incoherency modelling assumptions on SSI responses are reviewed. Both stochastic simulation (SS) approach and deterministic SRSS approaches implemented in conjunction with SASSI methodology are considered. The rigorous SS approach is implemented only in the ACS SASSI software, while the simplified, deterministic SRSS approach is also implemented in other SASSI methodology software.

Effects of Limited Number of Coherency Modes of SSI Analysis Runtime and Accuracy

To limit the computational efforts, SRSS is typically used with a reduced number of coherency matrix modes. For the RB sticks with rigid foundations as used in the 2007 EPRI validation studies (Short et al., 2007), the SRSS approach with only 10 coherency modes provided reasonable results. This is due to the effect of the kinematic SSI that for the rigid foundations filters out all the coherency matrix higher-order modes, except those that are closely to the rigid-body mode shapes. However, for a realistic FEA models with elastic foundations, tens, and sometime up to hundreds of coherency matrix modes are required for achieving a reasonable convergence for all locations, as defined by the 90% convergence coherency mode contribution criterion in equation 12.

The number of coherency modes impacts severely on the SRSS approach runtime and accuracy. Typically, the SRSS approach requires a restart SSI analysis for each coherency mode and direction. Thus, the computational analysis runtime for the SRSS approach increases linearly with the number of incoherency modes. If 40 coherency modes are required for the SRSS approach to obtain reasonable converged results, applicable to the three input directions, X, Y and Z, the overall incoherent SSI runtime will include *120 SSI restart analysis runs.* This is computationally prohibitive. Using the ACS SASSI SS approach with 20-25 stochastic simulations in a single run (that might twice longer than regular single run with one seismic load vector input) is about 50-60 times faster than the SRSS approach with 40 coherency modes! Moreover, the SRSS approach with 40 coherency modes does not necessarily ensure a reasonable accuracy for all ISRS locations within a R/B complex as shown in next section.

A reduced number of coherency modes has also a significant impact on the incoherent SSI response accuracy. Figure 12 shows computed ISRS results by the SS approach for a R/B complex FE model with flexible mat with 186 interaction nodes using 10, 20, 50 and 186 coherency modes. It should be noted that using 10 modes the incoherent ISRS are accurate only up to 10 Hz. Also, using a large number of 50 coherency modes still could provide significant error of 30%-40% in high frequency range.

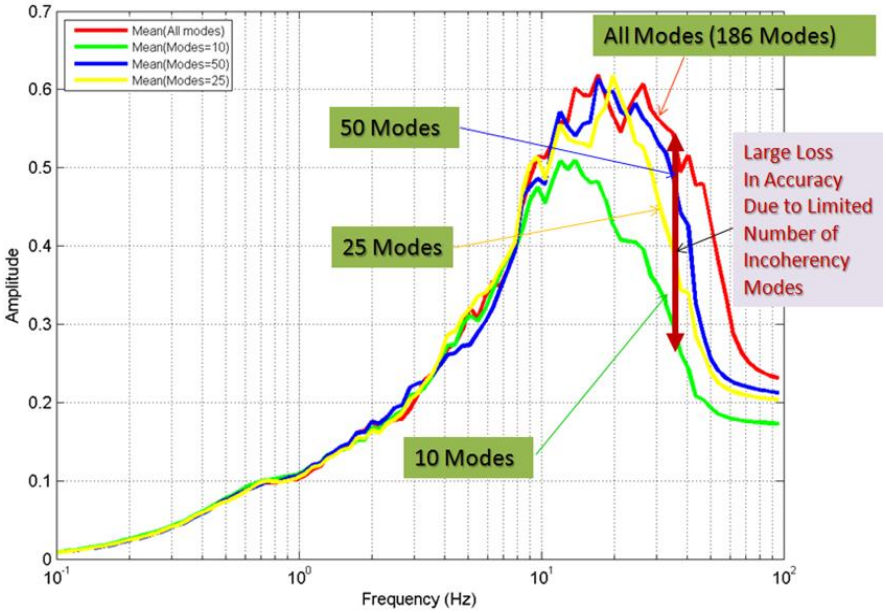

Figure 12 Incoherent ISRS Computed at the Basemat of the NI Complex

Figure 13 table shows the variation of the cumulative mode contribution with frequency for 10 coherency modes (as recommended in the SASSI2010 manual) for a basemat with similar sizes with the AP1000 NI foundation (Ghiocel, 2013). Such information is provided in the ACS SASSI HOUSE module output for incoherent analysis. It should be noted that above the 10 Hz frequency the cumulative mode contributions go below 90%. For the 40 Hz frequency, the cumulative mode contribution is only 16.31% for horizontal motion components and 21.74% for vertical motion components. This is explains the large underestimation of the computed ISRS in the high-frequency when only 10 coherency modes are used, as illustrated in Figure 12 (Ghiocel, 2013, 2014).

*** CUMULATIVE MODAL MASS/VARIANCE(%) *** **2007 Abrahamson Rock Site Model**

Frequency =	0.098	Horizontal =	100.00%	Vertical =	100.00%
Frequency =	1.562	Horizontal =	100.00%	Vertical =	99.97%
Frequency =	3.125	Horizontal =	99.94%	Vertical =	99.75%
Frequency =	4.688	Horizontal =	99.69%	Vertical =	99.20%
Frequency =	6.250	Horizontal =	98.90%	Vertical =	98.09%
Frequency =	7.812	Horizontal =	97.01%	Vertical =	96.00%
Frequency =	9.375	Horizontal =	93.55%	Vertical =	92.59%
Frequency =	10.938	Horizontal =	88.54%	Vertical =	87.93%
Frequency =	12.500	Horizontal =	82.47%	Vertical =	82.46%
Frequency =	14.062	Horizontal =	75.90%	Vertical =	76.67%
Frequency =	15.625	Horizontal =	69.31%	Vertical =	70.92%
Frequency =	17.188	Horizontal =	63.02%	Vertical =	65.45%
Frequency =	18.750	Horizontal =	57.20%	Vertical =	60.37%
Frequency =	20.312	Horizontal =	51.92%	Vertical =	55.74%
Frequency =	21.875	Horizontal =	47.19%	Vertical =	51.55%
Frequency =	23.438	Horizontal =	42.99%	Vertical =	47.79%
Frequency =	25.000	Horizontal =	39.26%	Vertical =	44.40%
Frequency =	26.562	Horizontal =	35.96%	Vertical =	41.37%
Frequency =	28.125	Horizontal =	33.04%	Vertical =	38.65%
Frequency =	29.688	Horizontal =	30.42%	Vertical =	36.20%
Frequency =	31.250	Horizontal =	28.04%	Vertical =	34.00%
Frequency =	32.812	Horizontal =	25.81%	Vertical =	32.01%
Frequency =	34.375	Horizontal =	23.63%	Vertical =	30.21%
Frequency =	35.938	Horizontal =	21.37%	Vertical =	28.57%
Frequency =	37.500	Horizontal =	18.93%	Vertical =	27.09%
Frequency =	39.062	Horizontal =	16.31%	Vertical =	25.74%

Figure 13. Cumulative Mode Contributions for Different Frequencies for 10 Coherency Modes

The analyst could consider an increasing number of modes and identify the frequency at which the 90% mode contribution criterion is reached (for 10 Hz is Figure 13). By tracking the number of required modes for which the 90% mode contribution is reached a relationship between the number of coherency modes and frequency can be established. However, the mode contribution criterion is based on global mode contribution, so that local modes with small contribution could be lost. A missed local coherency mode can affect severely the ISRS amplitude at a certain location, as shown in Figure 14.

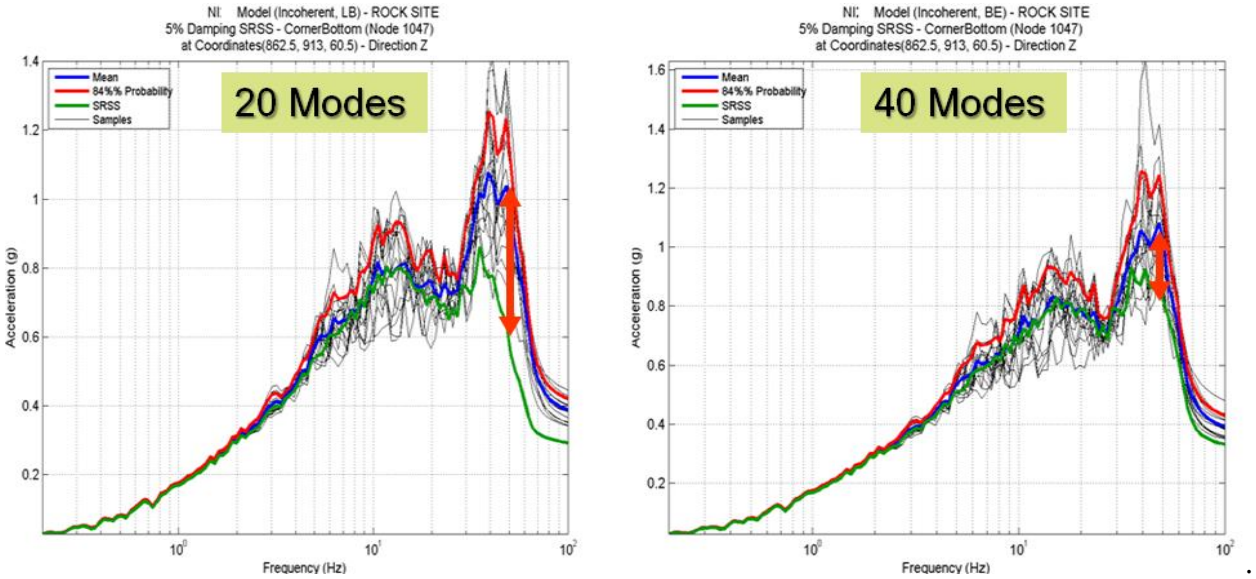

Figure 14 Effect of Number of Coherency Modes on Mean Incoherent ISRS Computed Using SRSS Approach; Incoherent SS Approach (blue) and SRSS Approach (green)

Similar to the SRSS approach applied to structural vibration modes, the SRSS approach applied to coherency modes neglects the effects of response phasing (or correlation) for the closely spaced modal responses. Due to this neglect, the SRSS approach could produce sometimes highly unreasonable results for complex FE models with elastic foundations for which many closely spaced coherency modes may contribute to the overall incoherent SSI response, especially at higher frequencies and in the vertical direction that is the most flexible direction of the foundation baseslab (as mentioned in new ASCE 4-16 standard, Section 5).

Effects of Neglect of Complex SSI Response Phasing

Basically, the stochastic simulation (SS) approach with no phase adjustment is identical with the standard Monte Carlo simulation approach (most world-wide accepted approach for modeling random phenomena in all engineering fields) applied to evaluate the motion incoherency effects on the SSI and SSSI responses.

The neglect of complex response phasing can affect the SSI responses. A simple example is provided in Figure 15 when a two support elastic beam is excited by a coherent harmonic motion with zero differential phase between the two input motions, and an incoherent harmonic motion with non-zero differential phase between the two input motions. It should be noted that coherent input excites only the 1st symmetric mode of the beam, while the incoherent motion excites both the 1st symmetric mode and the 2nd antisymmetric mode. Thus, the neglect of the motion differential phasing between two supports changes the dynamic system behaviour. These phasing effects on the SSI dynamic system response are not captured by the zero-phasing approaches.

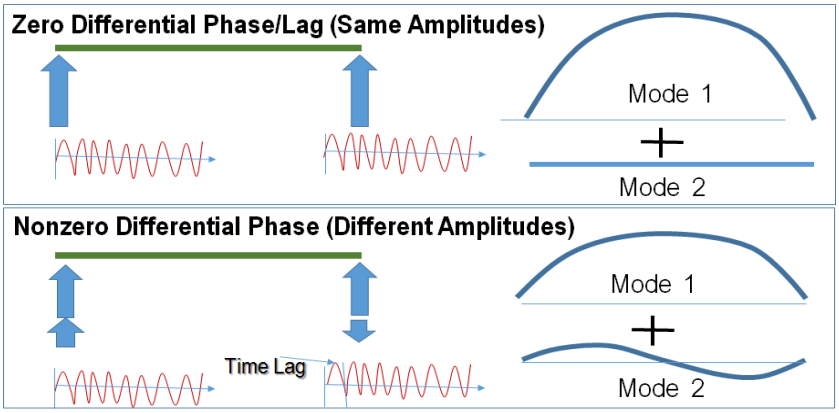

Figure 15 Effects of Coherent vs. Incoherent Inputs on Beam Dynamic Response

The effects of the SSI complex response phasing on a large-size R/B complex foundation motion is shown in Figure 16. Figure 16a shows the SSI response of the R/B basemat for the zero-phasing complex response assumption (incorrect mathematical modeling, intrusion in the SSI physics), while Figure 16b shows the SSI response of the same basemat for the realistic, random phasing complex response assumption (correct mathematical modelling, no intrusion in the SSI physics). It should be noted that the incoherent waves with larger wavelengths are basically non-existent for the zero-phasing complex response. Also, the zero-phase assumption produces a much noisier, quite artificial incoherent response. This makes the SSI motion for the zero-phasing assumption both less incoherent and less realistic.

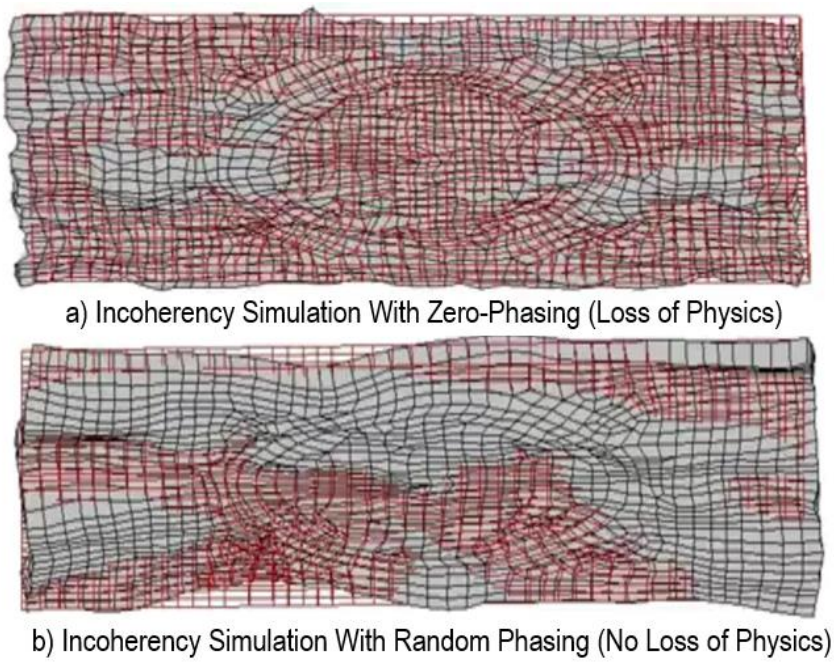

Figure 16 Effects of Zero-Phasing Assumption on Incoherent SSI Motion of RB Complex Basemat

Figure 17 shows the coherent and incoherent ISRS results obtained the a large-size RB complex using the rigorous SS approach with no phase adjustment (Simulation Mean, as the reference approach) versus the approximate SRSS and SS approaches with complex response zero-phase assumption. The effect of

phase-zeroing is highly conservative in this case since the input motion is less incoherent that it should be (shown in Figure 16).

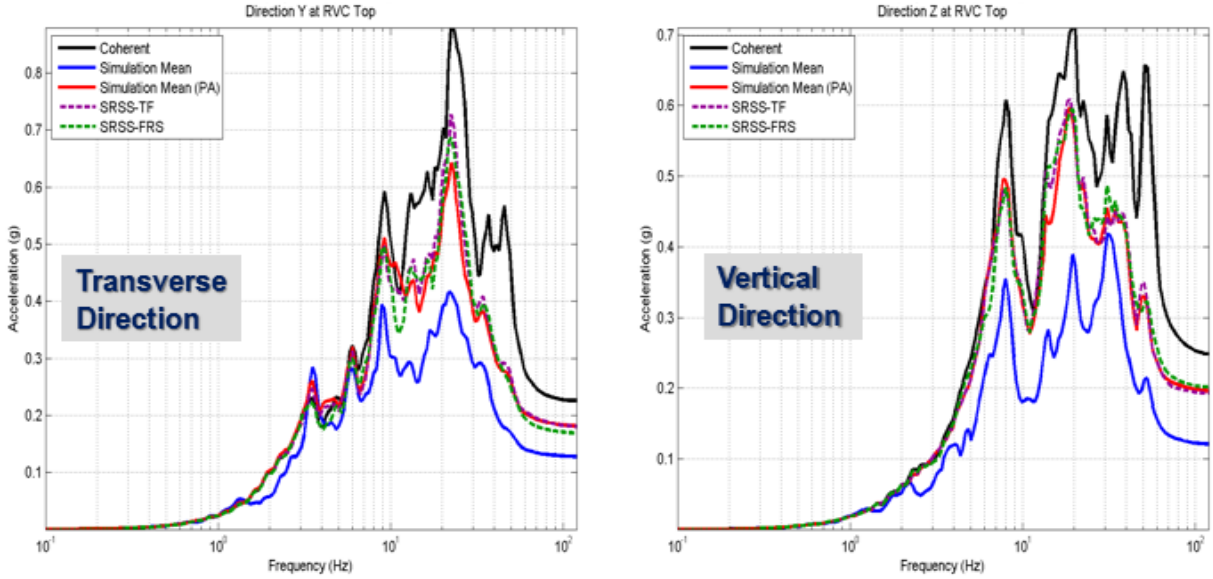

Figure 17 Effect of Complex Response Phase Zeroing on ISRS of RB Complex at RVC Top; Simulation Mean with No Phase Adjustment (blue solid), Simulation Mean (PA) with Phase Adjustment (red solid), and the SRSS approach (green and magenta dotted)

The phase adjustment not always produces conservative ISRS. There are some situations when the phase adjustment produces much smaller ISRS results than the no phase adjustment (Ghiocel, 2015, 2016).

Specific Embedment Modelling Issues

The use of deterministic SRSS approach with zero-phase for embedded models provides an arbitrary sign for the coherency modes. Figure 18 shows the contour plots for the coherency mode #9 at 11.72 Hz for a rectangular excavation volume. The two plots correspond to identical models that have different interaction node numbering. The differences between the two contour plots are due to the interaction node numbering that is different.

The eigen-decomposition of the coherency matrix for the two identical FE model produces the identical eigen-values and eigen-vectors for each embedment level, but not necessarily the eigen-vectors will have the same signs. Thus, for different interaction node numbering, the eigen-vector signs might randomly change. Thus, for the deterministic SRSS approach the mode signs can be assigned arbitrarily to be either 1 for zero value phase or -1 for 180 degree phase.

There is no physics-based criterion that can be imposed to control the mode sign. This lack of mode sign stability is due to the deterministic phase value limitation to only two values 0 or 180 degrees, i.e. + or – signs. This could affect largely the SSI results for a given coherency mode.

Figure 19 shows the significant effect of the coherency mode #1 sign change on the complex SSI response amplitude, in particular on the ATF amplitudes.

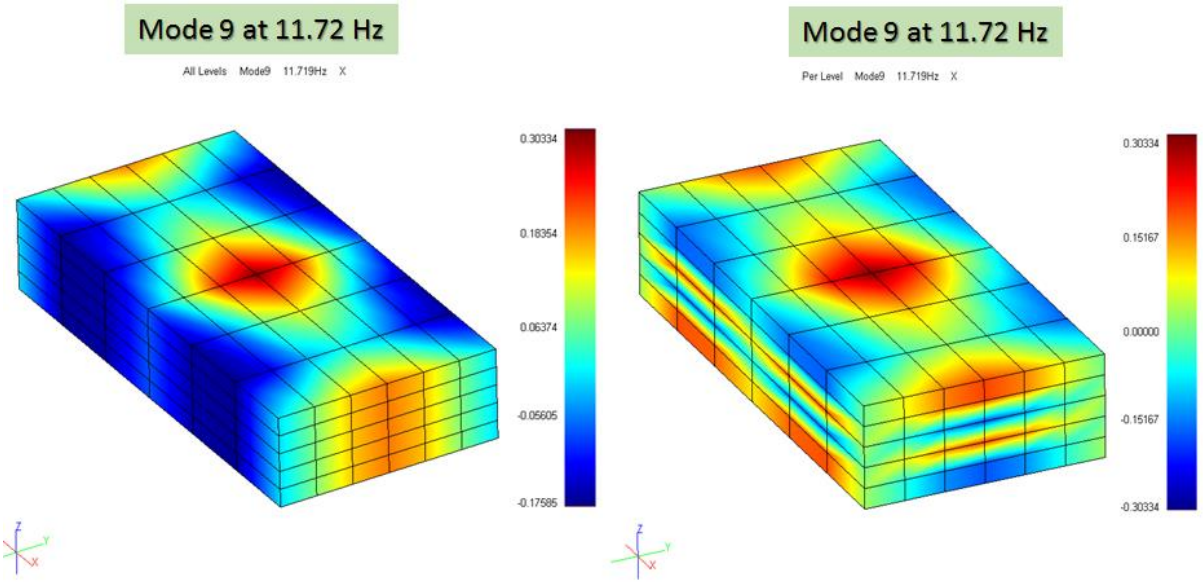

Figure 18 Effect of Interaction Node Numbering on Coherency Mode Signs for Embedded Models

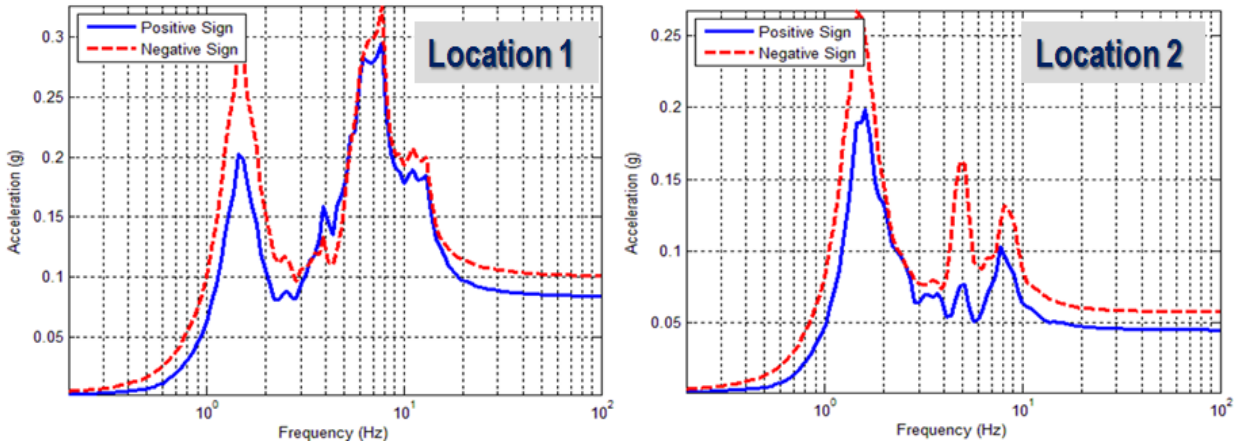

Figure 19 Effects of Mode 1 Sign Change on Acceleration Transfer Function (ATF) Amplitudes at Two Locations Within Excavation Volume

Effects of Motion Coherency Directionality

Typically the effect of motion directionality does not influence much the incoherent SSI response for rock sites, as shown in Figure 20 for a nuclear R/B complex at basemat level.

The ISRS plots show also results obtained using the Stochastic Simulation approach with phase adjustment (conventional approach) with alpha directional factor equal to 0.50, 0.10 and 0.90 vs. the SRSS approach with 40 coherency modes (Ghiocel, 2016).

The result comparison in Figure 20 indicates that the motion incoherency directionality has only limited effects on the ISRS results for both the horizontal and vertical directions.

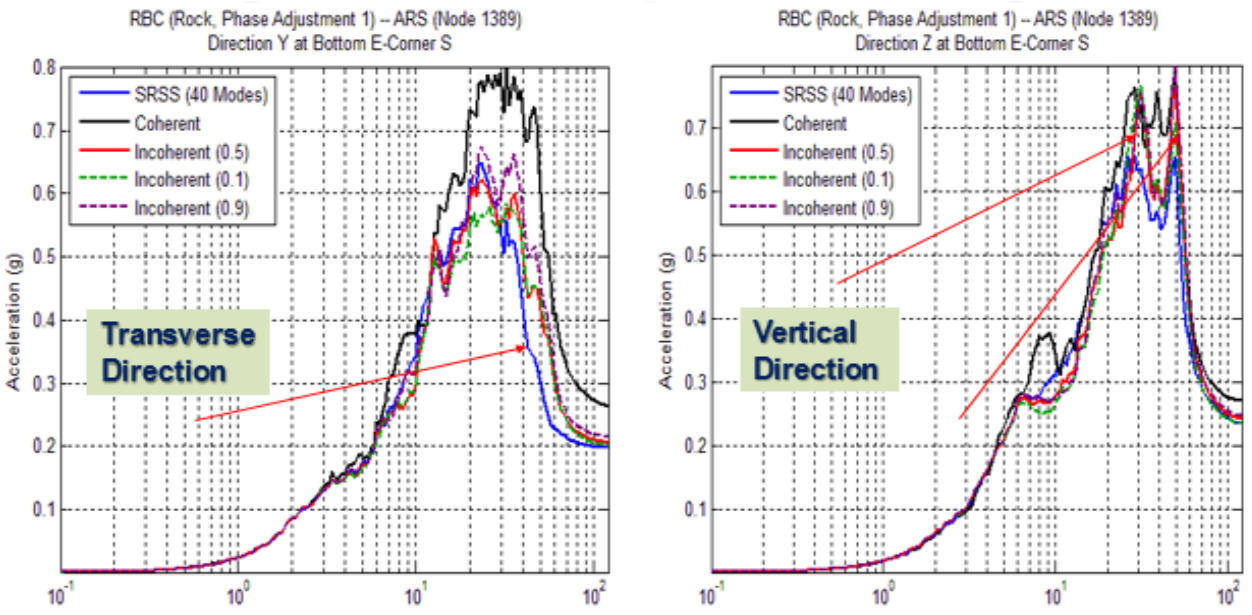

Figure 20. The Effect of Motion Incoherency Directionality on R/B Complex ISRS at Basemat

Effects of Incoherent Seismic Load Randomization for Surface and Embedded Structures

The implementation of motion incoherency within the SASSI framework is related to the modification of the seismic load vector used for SSI analysis using the FFL approach or the FFM approach as discussed in the previous section. Here, some quantitative comparisons are provided based on the ACS SASSI SS approach without phase adjustment (theoretically exact approach).

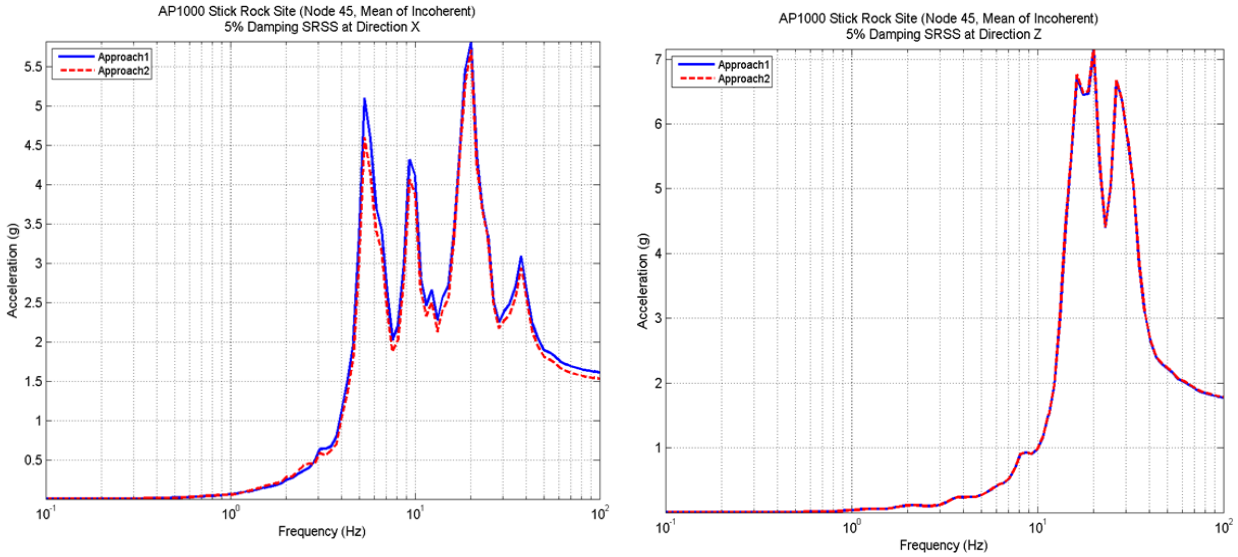

Figure 21 Incoherent ISRS Comparison Between FFL (blue) and FFM (red) Approaches at Top of EPRI AP1000 CIS (Node 45) for Horizontal and Vertical Directions

Figure 21 shows a comparison of the ISRS computed with the FFL and FFM approaches for the EPRI AP1000 stick surface SSI model used in 2007 EPRI studies (Short et al., 2007). Only minor differences are observed for horizontal direction. However, if the ISRS comparison is made for a large-size, surface

RB complex FE SSI model with an elastic basemat, the differences are more visible. The FFL approach provides again slightly larger ISRS for the horizontal direction as shown in Figure 22. It should be noted that the RB basemat mesh was quite a nonuniform mesh in horizontal direction that could also slightly affect this ISRS comparison.

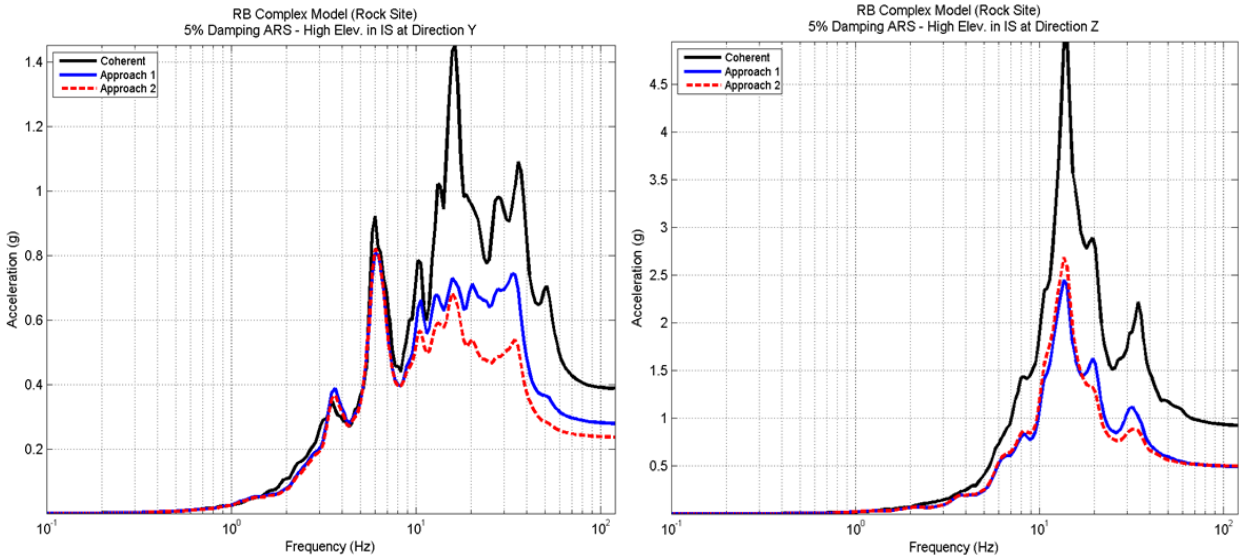

Figure 22 Coherent (black) vs. Incoherent ISRS Using FFL (blue) and FFM (red) Approaches at Top of RB Complex Internal Structure for Horizontal and Vertical Directions

Next, the ISRS comparison for the FFL and FFM approaches is made for embedded models in the context of using either the Flexible Volume (FV) method or the Modified Subtraction Method (MSM or FI-EVBN). Figure 23 shows an instant motion amplitude at the same time step for the excavated soil of a RB complex with 40ft embedment using the FV method (left) and the MSM method (right). It should be noted that the excavated soil motion indicate a slightly larger randomness in the scattered waves for the FV method in comparison with the MSM method.

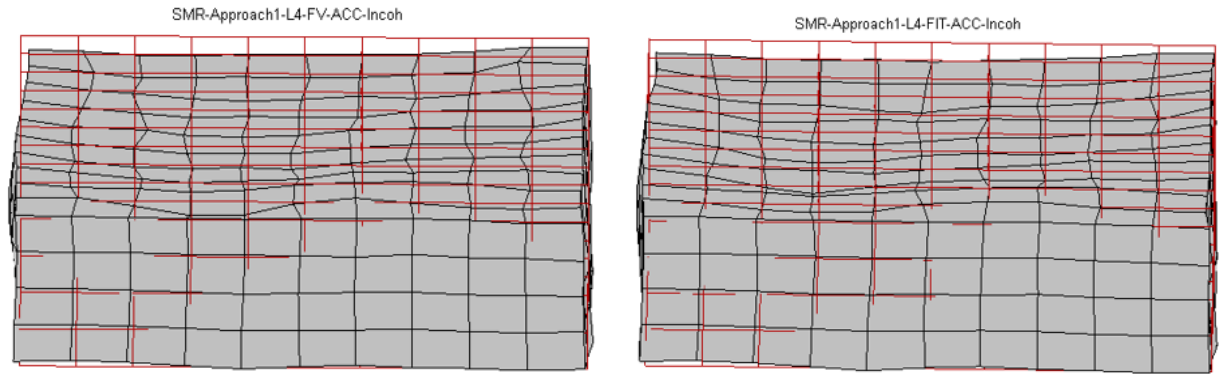

Figure 23 Excavated Soil Acceleration Motion at Selected Instant; FV (left) and MSM (right)

The incoherent ISRS results for two RB complex SSI models with two embedment levels of 40ft and 140ft, respectively, are compared. The comparisons include four cases, FFL-FV, FFL-MSM, FFM-FV and FFM-MSM. Figure 24 shows the ISRS computed for the RB complex with 40ft embedment. Reasonable, reduced differences are noted between the four cases.

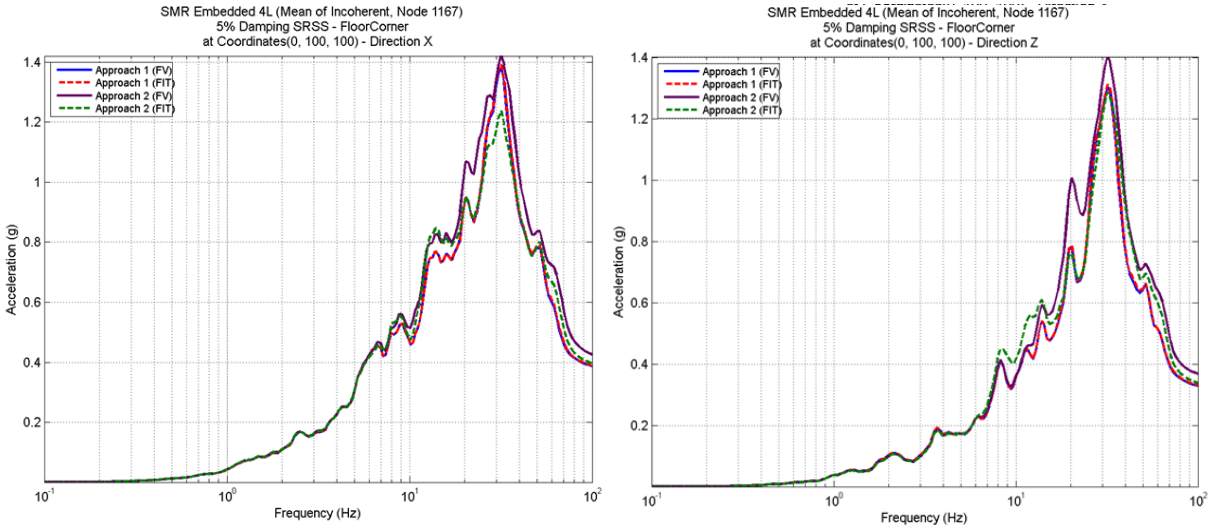

Figure 24 Incoherent ISRS for RB Complex with 40ft Embedment at Elevation 100 ft Above Ground; FFL-FV (blue solid), FFL-MSM (red dotted), FFM-FV (magenta solid), and FFM-MSM (green dotted)

Figure 25 shows the incoherent ISRS computed for the SMR complex with a 140ft embedment at the roof level. It should be noted that the ISRS computed for the four SSI analysis cases are relatively close, except for the FFM-MSM case that indicate a larger ISRS in high-frequencies, apparently with a numerical unstable amplification, especially for the vertical direction. Thus, it appears the FFM-MSM approach is slightly more unstable than the FFL-MSM approach.

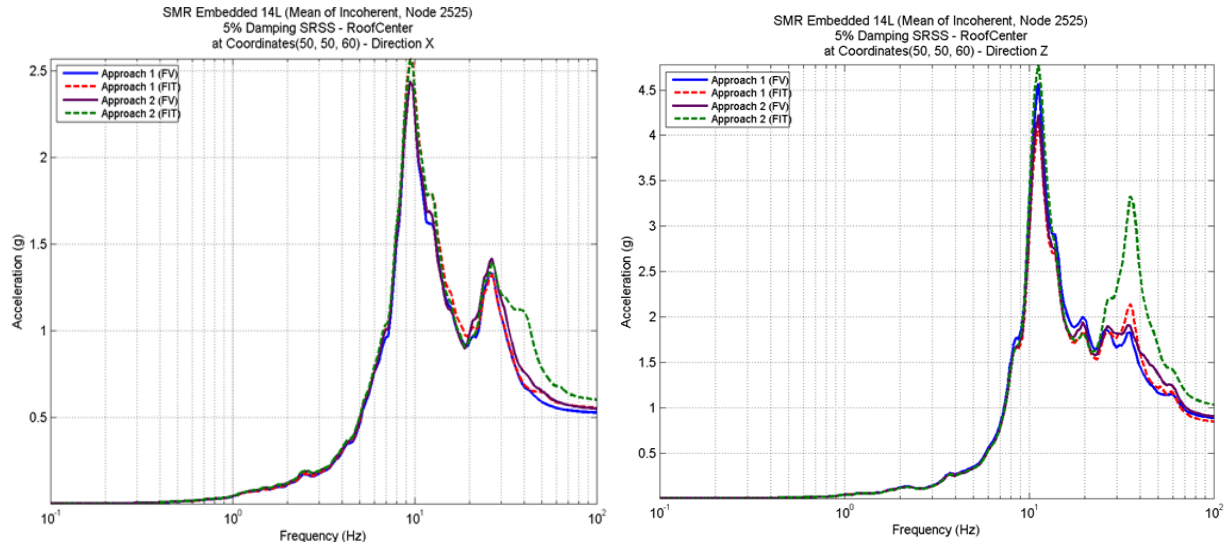

Figure 25 Incoherent ISRS for RB Complex with 140ft Embedment at Elevation 60ft Above Ground; FFL-FV (blue solid), FFL-MSM (red dotted), FFM-FV (magenta solid), and FFM-MSM (green dotted)

MOTION INCOHERENCY EFFECTS ON SSI AND SSSI RESPONSES

The incoherent motion in the free-field is described mathematically by a 3D wave stochastic field that is simulated based on the stochastic models developed based on real record statistical database. The coherent motion in free-field is described mathematically by a 1D wave propagation that generates a

"rigid body" motion in the horizontal plane. Thus, incoherent motion produces soil differential motions under foundations, while coherent motion produces no soil differential motions under foundations.

The motion incoherency has significant effects on the SSI responses of nuclear structures. Figure 26 shows a sketch that explains the difference between the coherent and incoherent soil motions on a stiff or flexible foundation/structure. Figure 26a shows the horizontal motion, while Figure 26b shows the vertical motion. The sketched plots compare the time moment of the maximum acceleration distribution of the coherent motion with the acceleration distribution of the incoherent motion. It should be noted that for coherent motion the accelerations can be maximum at the same time moment, while for incoherent motion the accelerations can't be maximum at the same time. The motion incoherency effects reduce the translational accelerations of the foundation/structure, and introduce rotational accelerations that do not exist under coherent motion. This is valid for the structure base motion, but also for the inertial forces that excite dynamically the structure.

The motion incoherency effects also increase with the frequency and the separation distance between point locations, or in other words increase with the foundation size.

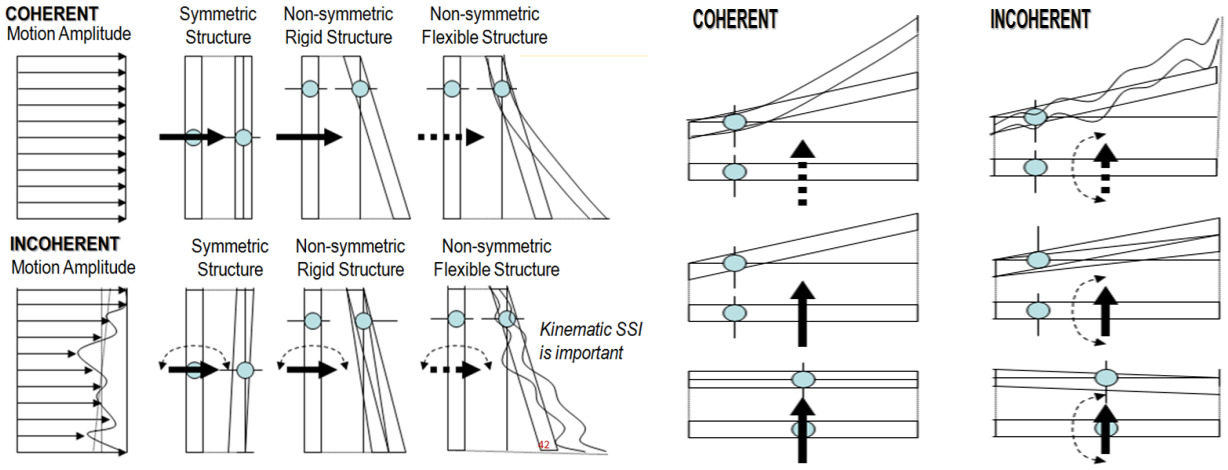

a) Horizontal Motion Component b) Vertical Motion Component

Figure 26 Coherent vs. Incoherent SSI Response Motions for Rigid and Flexible Foundation

The typical motion incoherency effects on the seismic SSI and SSSI responses of nuclear structures are as follows (Ghiocel, 2013, 2014, 2015, 2016):

1) The motion incoherency effects could decrease significantly the ISRS spectral peaks that correspond to translational vibration modes, but may increase ISRS peaks that correspond to rotational vibration modes. Since the incoherency effects increase with frequency and foundation size, the incoherency effects will be larger in higher frequency ranges and larger foundation sizes. Typically, the motion incoherency reduces significantly the high-frequency ISRS responses due to the translational vibration modes, but also amplifies any torsional or rocking modes, both local and global. It should be noted that incoherent ISRS could show new significant ISRS spectral peaks that are not visible in the coherent ISRS. This is due to the fact that the incoherent seismic inertial load on the structure is much less uniform and it excites much more the non-symmetric vibration modes both global and local.

2) Under the incoherent motions, the kinematic SSI effects are much larger than used the coherent motions. The foundation stiffness plays also an important role on the foundation behavior under incoherent differential motion, since the foundation stiffness impacts largely on the kinematic SSI

effects. Under incoherent motion the foundations are excited by differential soil motions that could produce much larger bending effects in the foundation walls and baseslabs than under coherent motion.

3) Motion incoherency could increase significantly the local the soil pressure variations on the foundation walls and mats.

4) The vertical differential motions at the basemat level are transmitted through the structure up to the building roof. This is due the fact that the basemat stiffness is much more reduced in vertical direction. This implies that the vertical differential structural displacements, including the locations of the supports of multiple-supported nuclear systems, could increase significantly.

5) Motion incoherency affects the SSSI coupling response effects, and by this could affect significantly the ISRS and the seismic soil pressures. Motion incoherency usually amplifies the dynamic coupling between buildings, since the basemat motions of the coupled buildings are different, depending on foundation sizes. The SSSI effects could produce significant new spectral peaks in the SSSI ISRS that did not exist in the standalone SSI ISRS. These new SSSI ISRS peaks are a result of the some new vibration SSSI modes that are excited much more by the incoherent seismic inertial forces and foundation displacements than the coherent seismic load inertial forces and foundation displacements.

CONCLUSIONS

The seismic motion incoherency is a real phenomenon that affects at certain level the SSI responses of nuclear structures for both the soil and rock site conditions. It is always a good engineering judgement to evaluate the effects of motion incoherency on the SSI and SSSI responses and then compare them with "traditional" simplified coherent responses. Incoherency effects are both favorably and unfavorably depending on the SSI or SSSI response quantity of interest.

It is also extremely important to use sufficiently accurate incoherent SSI approaches that provide results based on a physics-based modeling that are also consistent with the observed reality. We strongly recommend to use as a reference approach the Stochastic Simulation (SSI) approach that is based on the standard Monte Carlo simulation, the most robust stochastic approach in engineering.

REFERENCES

Abrahamson, N. (2007)."Effects of Spatial Incoherence on Seismic Ground Motions", Electric Power Research Institute, Palo Alto, CA and US Department of Energy, Germantown, MD, Report No. TR-1015110, December 20

Deodatis, G., (1996). "Non-Stationary Stochastic Vector Processes: Seismic Ground Motion Applications", Probabilistic Engineering Mechanics, Vol. 11, 149–168, 1996.

Ghiocel Predictive Technologies, Inc. (2017). "ACS SASSI - An Advanced Computational Software for 3D Dynamic Analyses Including SSI Effects", ACS SASSI Version 3.0 User Manuals, December

Ghiocel, D.M., (2016). "Critical Modeling and Implementation Aspects for Seismic Incoherent SSI Analysis of Nuclear Structures with Surface and Embedded Foundations for Rock and Soil Sites", 2-Day U.S. Department of Energy Natural Phenomena Hazards Meeting, Germantown, MD, USA, October 18-19, 2016, Session on "Soil-Structure Interaction"

Ghiocel, D.M., (2015). "Seismic Motion Incoherency Effects on Soil-Structure Interaction (SSI) and Structure-Soil-Structure Interaction (SSSI) of Nuclear Structures for Different Soil Site Conditions", the SMiRT23 Conference for NPP Structures, August

Ghiocel, D.M. (2014). "Effects of Seismic Motion Incoherency on SSI and SSSI Responses of Nuclear Structures for Different Soil Site Conditions", 2-Day U.S. Department of Energy Natural Phenomena Hazards Meeting, Germantown, MD, USA, October 21-22, 2014, Session on "Soil-Structure Interaction"

Ghiocel, D.M. (2013).”Comparative Studies on Seismic Incoherent SSI Analysis Methodologies”, the SMiRT22 Conference Proceedings, Division V, San Francisco, California, August 18-23, 2013

Ghiocel, D.M. (2007). “Stochastic and Deterministic Approaches for Incoherent Seismic SSI Analysis as Implemented in ACS SASSI Version 2.2, The Appendix C of the “Validation of CLASSI and SASSI to Treat Seismic Wave Incoherence in SSI Analysis of Nuclear Power Plant Structures”, Electric Power Research Institute, Palo Alto, CA and US Department of Energy, Germantown, MD, Report No. TR-1015111, November 30

Ghiocel, D.M. (1996) " On Accuracy of Coherency Spectrum Estimation for Broad and Narrow Band Stationary Processes", the Proceedings of the 7th International Conference on Applied Statistics and Probability, Paris, July, 1995

Schneider J.F., Stepp, J.C. Stepp and Abrahamson, N.A. (1992).”The Spatial Variation of Earthquake Ground Motion and Effects of Local Site Conditions”, Proceedings on the 10th World Conference on Earthquake Engineeing, Madrid, Spain

Short, S.A., G.S. Hardy, K.L. Merz, and J.J. Johnson. (2007). “Validation of CLASSI and SASSI to Treat Seismic Wave Incoherence in SSI Analysis of Nuclear Power Plant Structures”, Electric Power Research Institute, Palo Alto, CA and US Department of Energy, Germantown, MD, Report No. TR-1015111, November 30

Svay, A., Zentner, I., Clouteau, D., Cottereau, J.(2016) “Spatial Coherency Analysis of Seismic Ground Motions from a Rock Site Dense Array Implemented during the Kefalonia 2014 Aftershock Sequence”, LOSSVAR Seminar, EDF Lab, Pais-Saclay, August 26.

Tseng, W. and Lilhanand M. (1997). “Soil-Structure Interaction Analysis Incorporating Spatial Incoherence of Ground Motions”, Electric Power Research Institute, Palo Alto, CA and US Department of Energy, Germantown, MD, Report No. TR-102631, 1997

Zerva, A. (2008). “Spatial Variation of Seismic Ground Motions: Modelling and Engineering Applications”, CRC Press, Taylor & Francis, Boca Raton, London, New York